ICMIEE22-057

Simulation of acoustic emission signal and its verification on a resonant sensor

Arif Abdullah Rashid[1,], Md. Tawhidul Islam Khan[2], Nazmush Sakib[3], Tokumaru Nanami[4]*
[1] Graduate School of Science and Advanced Technology, Saga University, 1 Honjo-machi, Saga 840-8502, JAPAN
[2] Faculty of Science and Engineering, Saga University, 1 Honjo-machi, Saga 840-8502, JAPAN
[3] Department of Advanced Health Science, Saga University, 1 Honjo-machi, Saga 840-8502, JAPAN
[4] Department of Mechanical Engineering, Saga University, 1 Honjo-machi, Saga 840-8502, JAPAN

ABSTRACT
In this paper, the simulation of AE wave has been modelled based on the peak sensitivity characteristics of a resonant piezoelectric AE sensor. For the generation of AE wave, a vertical point load has been applied on a traction free aluminum (A5052) surface. The resonance AE sensor collects the vertical response of P- wave, S wave and Rayleigh wave as the AE displacement wave. The displacement wave has been transformed into AE electrical signal by the sensor. The transfer function has been developed from the peak sensitivity value and the sensitivity curve of the R15α sensor. The sensor sensitivity curve has been evaluated by the concept of face-to-face calibration method. The transfer loss of the AE signal has been determined based on the acoustic impedance of the propagation materials. The simulated AE signal is characterized based on two major AE parameters i.e., rise time and maximum amplitude. A model experiment has been performed on the aluminum block (500mm × 250 mm × 250mm) for the validation of simulation results. Both the simulated and the experimental AE waves were compared based on AE parametric analysis. The time of arrival (TOA) of the generated wave was determined by Akaike's information criterion (AIC) method. Significant characteristics of the rise time and the maximum amplitude with increment of source to sensor distance have been observed. The increment of rise time and the attenuation properties of maximum amplitude with the increase of source to sensor distance has been evaluated to validate the proposed AE model.

Keywords: Acoustic emission, homogenous material, vertical response function, resonant sensor, sensor transfer function

1. Introduction

Among various non-destructive testing available in the world, acoustic emission (AE) technique is globally used for the qualitative analysis of damage in structures and materials [1]. The anomaly which is arisen in a material due to variation of stress, develop strain energy and it travels through the body as elastic transient wave. This kind of wave is known as AE wave [2]. If a sensor is attached on the body, it will receive the AE wave in the form of electrical signal. Studying these signals will provide the knowledge about the characteristics of the damage of the body to prevent from significant failure. Its application is spreading in various engineering field for its dynamic monitoring capability. The PZT (lead zirconate titanate) sensors of various frequency range are commonly used for the detection of AE wave. This piezoelectric sensor converts the AE displacement waves into AE electrical signals. The AE acquisition device is used to visualize the signal in the amplitude (voltage) vs time (second) data and various AE parameters are determined from that data. A sample AE wave with its various important parameters is shown in Fig.1.

Presently large numbers of study are being carried out to generate numerical AE wave based on the prevailing AE theories [3]. The quantitative analysis is essential to implement this technique more preciously in damage forecasting and characterizing. With the proper knowledge of AE wave formation and propagation will increase the robustness of AE technique in various field of study. In this paper, the convolution integral in time domain is applied to numerical modelling of AE wave. The simulated AE wave is developed by a vertical load applied on the surface of an aluminum (A5052) block (500mm × 250 mm × 250mm). The P-wave, S wave and surface waves propagate through the material. The vertical response of these waves is collected by a resonant AE sensor attached on the aluminum surface. The peak sensitivity of the resonant AE sensor is considered to determine the transfer function of the AE displacement wave. The acoustic impedance of the materials is calculated to determine the transfer loss. A model AE experiment has been performed to validate the simulation results. The simulated and experimental AE waves have been compared based on AE parametric analysis. The time of arrival (TOA) of the generated

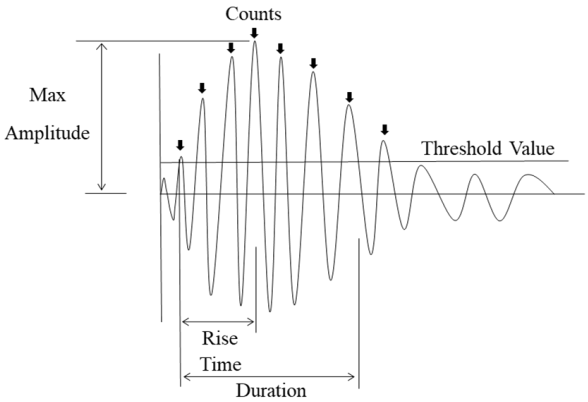

Fig.1 A typical AE wave and its various parameters

* Corresponding author. Tel.: +81-9096036286
E-mail addresses: aarashid93@gmail.com

wave has been determined by Akaike's information criterion (AIC) method. The rise time of AE wave has been calculated from the time to reach the maximum amplitude and TOA. Notable characteristics of rise time and maximum amplitude with change of source to receiver distance have been observed. This approach can be applied to generate AE wave quantitatively for any piezoelectric resonant AE sensor available for commercial use.

2. Theory of AE wave modelling on aluminum block

2.1 Displacement function of AE wave

For the modelling of AE wave formation and propagation, aluminum A5052 is regarded as the homogenous medium in our research. The properties of A5052 are listed in table 1.

Table 1 Properties of aluminum(A5052)

Density, ρ_{Al} (kg/m3)	Young's Modulus, E_{Al} (GPa)	Poisson's ratio, υ_{Al}
2680	69.3	0.33

The AE wave is generated due to change of stress in aluminum, and it travels through the body in the form of elastic wave. Let ***i*** component of vector displacement, u_i (***x***, ***t***) from ***x*** at time ***t*** is considered due to force along ***j.*** If an internal stress is formed in aluminum of density ρ_{Al}, the governing equation for wave motion is given as follows [4],

$$(\lambda_{Al}+\mu_{Al})u_{j,ji} + \mu_{Al}u_{i,jj} = \rho_{Al}\ddot{u}_i \quad (1)$$

The constant value of λ_{Al}, and μ_{Al}, are determined from the aluminum properties (Table 1). The Green's function, $G_{ij}(x_o,0; x,t)$ indicates the relation between the source $(x_o,0)$ and the detection point (x,t). It is also the response function along ***i*** direction due to a point load along ***j*** direction. The surface pulse on any material emits compressional spherical wave like that of any seismological wave. When it is detected, it has all the components along vertical, horizontal and radial directions. The sensor is attached normal to the aluminum surface. Therefore, the vertical component is considered in present paper. For a point source function $f_z(t)$ along Z-axis, Eq. (1) is expressed by the following equation [5],

$$u_z(x,t) = G_{zz}(x;t) * f_z(t) = \frac{d}{dt}\left[{G_{zz}}^S(x-x_0;t)\right] * [Ff_z(t)] \quad (2)$$

Here, $G_{zz}^S(x-x_o;t)$ is the response function due to unit step load and F is the magnitude of the load. The expression for the response function, G_{zz}^S for a unit step load along the Z-axis for dimensionless time, T and at a source to sensor distance, R and is shown below [6],

$${G_{zz}}^S(R,T) = \frac{C}{R}\begin{cases} \frac{1}{2}\left(1-\sum_{i=1}^{3}\frac{A_i}{\sqrt{|T^2-{m_i}^2|}}\right) & .5 < T < 1 \\ 1-\frac{A_1}{\sqrt{.25-T^2}} & 1 \le T < m_1 \\ 1 & T \ge m_1 \end{cases}$$

Where $A_i = \frac{\left({m_i}^2-\frac{1}{2}\right)^2\sqrt{|.25-{m_i}^2|}}{({m_i}^2-{m_j}^2)({m_i}^2-{m_k}^2)}$ and $i \neq j \neq k$ (3)

Here, C is a constant based on aluminum properties (Table 1) and m_i denotes the three roots of Rayleigh function. Here i is equal to 1, 2, 3. m_1 portrays the real Rayleigh root as well as the ratio of S-wave and Rayleigh wave velocities. The Rayleigh function, RF for aluminum is given below [7],

$$RF(m) = m^3 - 8m^2 + 16m - 8 = 0 \quad (4)$$

2.2 AE wave function from AE sensor

The dynamic motion of the AE wave is converted into electric signal by the piezoelectric AE sensor attached on the material surface. It is further processed to be displayed in the acquisition device. For the conversion, a transfer function of the sensor is required. The face-to-face calibration method has been applied for the determination of sensor sensitivity. For a known input sweep signal and output response the sensor system has been determined by the following relation:

$$Sys(f) = \frac{V_{out}(f)}{V_{in}(f)} \quad (5)$$

Here $Sys(f)$, $V_{out}(f)$ and $V_{in}(f)$ are all in frequency spectrum. The normalized magnitude with respect to the maximum response of the system is converted to dB (ref. 1 Volt/µbar) to represent the sensor sensitivity curve of the sensor system for a particular resonant sensor. To find the transfer function of the sensor the following equation is used [8]:

$$T_{PS}(t) = inverse\ fft\left[Sys(f) * 2\pi f_{PS} V_R 10^{\frac{dB_{PS}}{20}}\right] \quad (6)$$

Here, V_R is reference of the sensitivity curve, dB_{PS} is the peak sensitivity for AE sensor and f_{PS} is the peak sensitivity frequency of the sensor. The commonly used piezoelectric sensors have V_R value of 0 dB at 1 Volt/µbar. For the conversion to 0 dB at 1 Volt/(m/sec), a factor of 143.4dB is added to the peak sensitivity value in the Eq. (6) [8]. When a function generator is used to provide loads on the surface, there will be two transfer loss for the received AE signal. The first one is due to transfer of signal from the source actuator to the material and the second one is due to transfer of the signal from the material to receiver sensor. The T_{AI} is determined by the following equation [9],

$$T_{AI} = \left(1 - \left(\frac{Z_A - Z_{Al}}{Z_A + Z_{Al}}\right)^2\right)_{source} \cdot \left(1 - \left(\frac{Z_S - Z_{Al}}{Z_S + Z_{Al}}\right)^2\right)_{receiever} \quad (7)$$

Here, Z_A is the acoustic impedance of source actuator's material, Z_S is the acoustic impedance of receiver sensor's material and Z_{Al} is acoustic impedance of aluminum. The final AE wave amplitude function, $U(t)$ for a load function, $f_Z(t)$ is expressed in the time domain by the following equation [10],

$$U(t) = \frac{d}{dt}\left[{G_{zz}}^S(R,t)\right] * [Ff_z(t)] * T_{PS}(t) * T_{AI}$$
$$= {G_{zz}}^S(x - x_O; t) * [Ff_z(t)] * \frac{d}{dt}[T_{PS}(t)] * T_{AI} \quad (8)$$

Here, $T_{PS}(t)$ and T_{AI} are integrated in the Eq. (3) according to linear filter theory. The AE wave amplitude, $U(t)$ is received in voltage. Fig. 2 shows the representation of Eq. (8).

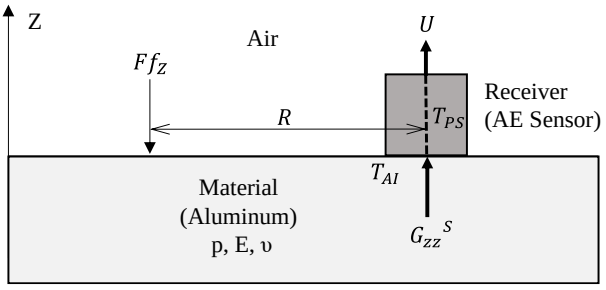

Fig.2 Schematics of AE wave generation

2.3 AE wave velocity

The received vertical AE wave in aluminum has distinct kinds of waves namely P-wave, S-wave, surface waves etc. Among the surface waves, the Rayleigh wave dominates due to high frequency-thickness, fd (fd>4MHz-mm) value for aluminum. The fd value is determined from the dispersion curve of Lamb wave for aluminum. The velocities of P-wave (V_P), S-wave (V_S) and Rayleigh wave (V_R) are determined from the aluminum properties (Table 1) by the following relations [11],

$$V_S = \sqrt{\frac{(1-2\upsilon_{Al})}{2(1-\upsilon_{Al})}} V_P = \frac{1+\upsilon_{Al}}{0.87+1.12\upsilon_{Al}} V_R$$

$$\text{where } V_P = \sqrt{\frac{E_{Al}(1-\upsilon_{Al})}{\rho_{Al}(1+\upsilon_{Al})(1-2\upsilon_{Al})}} \quad (9)$$

3. Simulation of AE wave

The AE wave amplitude function from Eq. (8) was simulated in MATLAB. The algorithm relied on some assumptions. Firstly, the generated wave flowed through the homogenous material uniformly. Since the material was homogenous, there was no attenuation of elastic energy inside the material. The AE sensor picked the uniform wave reading. Secondly, the frequency-thickness, *fd* value was high enough to reduce the probability of producing others surface waves except Rayleigh wave [12]. The P-wave, S-wave and Rayleigh wave were only generated on the surface. The effects due to reflected waves on the boundary surface were neglected. The flow diagram in Fig. 3 shows the algorithm of the AE wave simulation.

The time step, Δt was selected as 10^{-7} sec. From Eq. (9) the Rayleigh wave, P-wave and S-wave velocities were calculated. Using Eq. (3), the response curve was simulated at 16 different source to receiver distances, R (from 0.025 m to 0.4 m with an increment of 0.025 m). The input load was a burst sine function. The frequency and amplitude were 200kHz and 20 peak to peak volt respectively. The contact area with the material of the source actuator (diameter is 12 mm) was multiplied with the load magnitude to convert it to point load. A resonant R15α sensor having peak sensitivity -63 dB (in reference to 1 Volt/μbar) was considered. The $T_{PS}(t)$ was determined from the face-to-face calibration experiment and the properties of AE sensor by Eq. (6). The surface of both the source actuator and sensor was made of ceramic. So, using Eq. (7), the T_{AI} value equal to 0.51 was calculated. The preamplifier of 40dB gain was used in the simulation. It magnified the AE wave signal by 100 times. By incorporating all the values and convoluting according to Eq. (8), the simulated output of AE signal in voltage was generated.

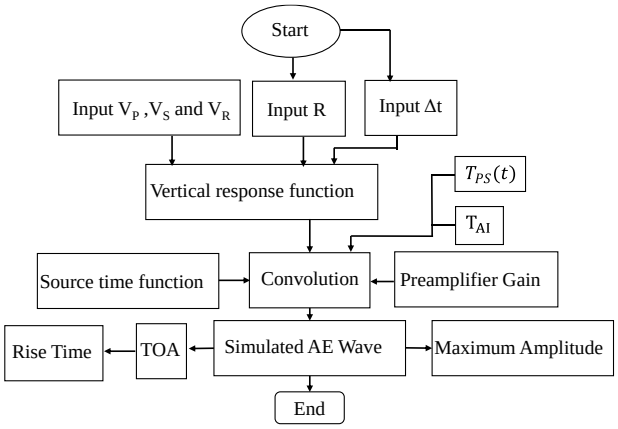

Fig. 3 Algorithm for AE wave simulation program

4. Experiment methodology

4.1 Sensor sensitivity curve evaluation experiment

The sensitivity curve of AE resonant sensor (Model: R15α 150 kHz resonant frequency, peak sensitivity -63 dB, 0 dB at 1 Volt/μbar, Physical Acoustics, USA) was determined by face-to-face calibration method. A function generator (Model: WF1973) was used to input a sweep sine signal (10kHZ-400kHz, 0.5 Vp-p) on the sensing surface of

the AE sensor. A wide band AE sensor (Model: AE-900S-WB, NF Corporation, Japan) was selected as the actuator. Before attaching with the acquisition system (Express-8 AE system, Physical Acoustics, USA) of the AE wave, the receiving AE sensor was combined with the pre-amplifiers (Model: 2/4/6) with 40 dB gain. The whole setup is shown in Fig. 10.

4.2 AE Validation experiment

A model experiment of AE wave generation was performed on an aluminum block (500mm × 250 mm × 250mm). The similar function generator and AE sensor were used for source initiation in this experiment also. An input sine signal of frequency 200kHz and amplitude 20 volts (peak to peak) was imparted on the aluminium block surface in burst mode. The R15α sensor was placed on the surface as the receiver of the generated AE signal. It was coupled with acoustic coupling gel. The pre amplifier of 40 dB gain was used before connecting to the acquisition system. The schematic diagram of the whole setup is demonstrated in Fig. 4. The threshold value was selected as 40 dB and the sample rate was 10 MSPS. The PDT (peak definition time), HDT (hit definition time), HLT (hit lockout time) and duration values were 200 microseconds, 400 microseconds, 400 microseconds and 99 milliseconds respectively. An analog filter of 100-400 kHz was considered. By varying the source to sensor distances, R with an increment .025 m up to .4 m, the load was applied on the surface. The calculated *fd* value was 50 MHz-mm. The AE data were collected by the sensors and along with the AEwin software. Thus, the collected data in the experiment were used for the comparison of the simulated data.

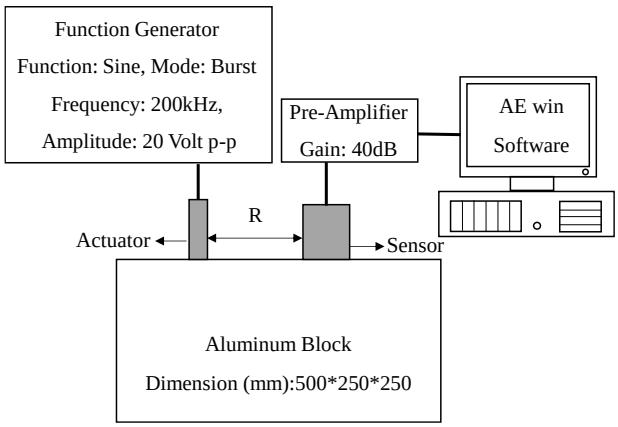

Fig. 4 The schematic diagram of the experimental setup

5. Results and discussion

5.1 Sensitivity curve for R15α sensor

According to Eq. (6) the sensitivity curve of the R15 alpha resonant AE sensor was determined and is shown by the Fig. 5. The frequency is along x axis and the sensor sensitivity is in dB (ref. 1 Volt/µbar). The resonant frequency resonant frequency is around 150 kHZ as shown in the figure.

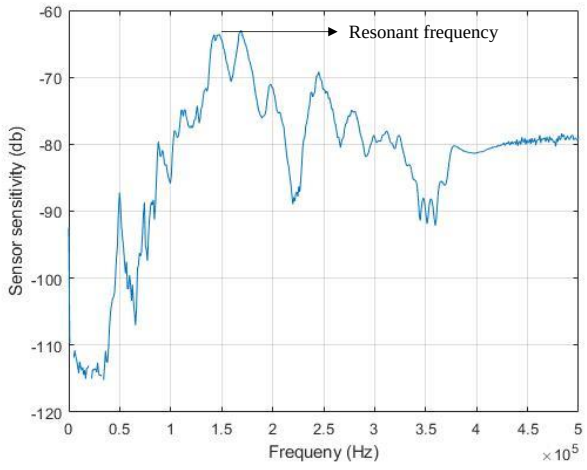

Fig. 5 The sensor sensitivity curve for R15α sensor

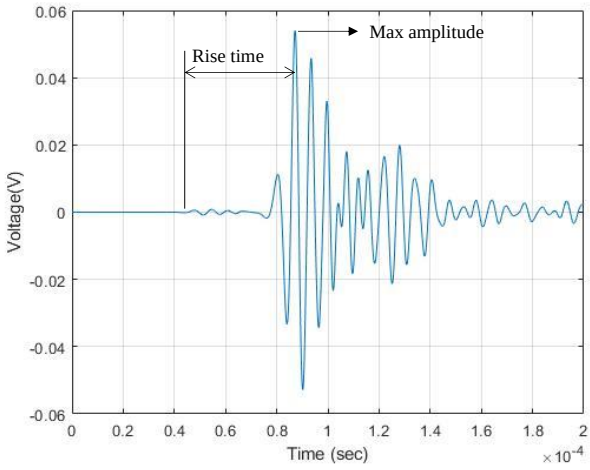

(a)

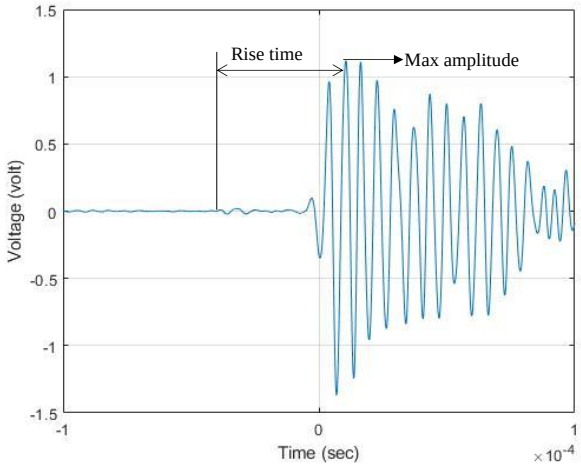

(b)

Fig.6 The sample AE at R=0.2 m is received from (a) simulation and (b) experiment

5.2 Comparison of simulated AE Wave with experiment

The simulated AE wave at R equal to 0.2m as sample wave was determined and shown by the Fig. 6a. The respective experimental AE wave was compared with it as given in Fig. 6b. The rise time and the maximum amplitude were presented for both the AE waves.

5.3 Rise time of AE wave

In this paper, Akaike's information criterion (AIC) method was used for picking the time of arrival (TOA) of the received AE signal. The TOA of the first wave picked by AIC was calculated with the increase of source to sensor distance, R. The rise time, RT was determined by subtracting the time to reach the maximum amplitude with TOA for both experimental and simulated AE waves. The analyzed results are shown in the Fig. 7. The rise time has been increased with the increase R. The wave requires more time to travel as the propagation distance increases. The similar trend was observed in both experimental and simulated AE signals. The average percent deviation of the experimental rise time with respect to simulated rise time was 9.06%. The simulation was executed based on the theoretical velocity. But there was variation of experimentally observed velocity at each measuring point with the theoretical velocity. This was considered to induce the overall deviation of the experimental rise time with the simulated rise time.

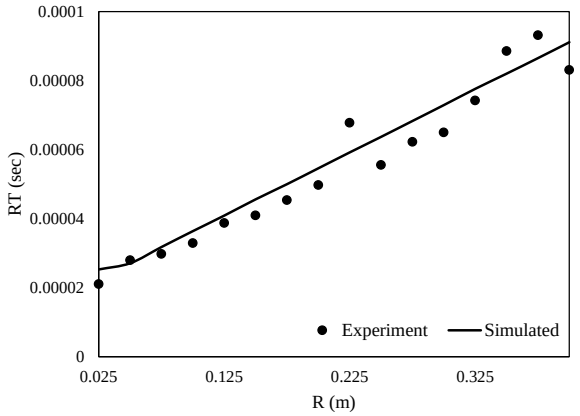

Fig. 7 The comparison of rise time (RT) with the increase of source to receiver distance (R) for both simulated and experimental AE wave

5.3 Maximum amplitude of AE wave

Next, the maximum amplitude of the AE signal was analyzed. With the increase of the source to receiver distances, the maximum amplitudes attenuated. This is known as the attenuation characteristics of the AE waves maximum amplitudes. Figs. 9a and 9b show the analyzed result of the experimental AE waves comparing with simulated AE waves. The trend of maximum amplitude for both the waves were analogous.

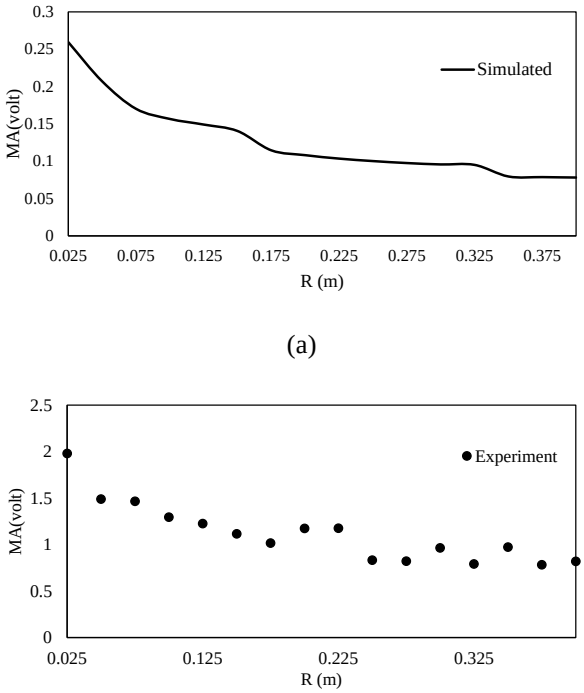

Fig.8 The attenuation properties of maximum amplitude (MA) with the increase of source to receiver distance (R) for both (a) simulated and (b) experimental AE wave

6. Conclusions

The generation of AE wave on an aluminum block has been developed based on convolution integral in time domain. The properties of the R15α sensor have been employed to evaluate the proposed transfer function due to peak sensor sensitivity curve. The transfer loss factor for acoustic impedance was also evaluated to define the loss of AE wave signal due to the change of the propagation medium. The simulated AE signal has been compared with the model experiment on the aluminum block. Two major parameters of AE wave were evaluated for both the simulated and the experimental AE waves. The characteristics of the rise time and the maximum amplitude have been presented with the increase of propagation distance (R). The increment of rise time has been perceived for both simulated and experimental AE waves. The attenuation property of maximum amplitude has been verified for both simulated and experimental AE waves.

This proposed approach is suitable to apply to any piezoelectric AE sensor, homogenous material and source function. Further work is going on to increase the robustness of this methods.

8. References

[1] Khan, M. T. I., Rashid, A. A., Hidaka, R., Hattori, N. and Islam, M. M., Fatigue crack analysis of ferrite material by acoustic emission technique,

Journal of Mechanical Engineering and Sciences, vol. 13 (2), pp. 5074-5089, 2017.
[2] Ohtsu, M., The history and development of acoustic emission in concrete engineering, *Proc. of JSCE*, vol. 496 (24), pp. 9-19, 1995.
[3] Aki, K. and Richards, P. G., Quantitative seismology, University science books, Mill Valley, Ed. 2, California, 2002.
[4] Ohtsu, M. and Ono, K., A generalized theory of acoustic emission and green functions in a half space, *Journal of Acoustic emission*, vol. 3, pp. 27-40, 1984.
[5] Grosse, C. U., Ohtsu, M., Acoustic Emission Testing, (Eds.) Springer-Verlag Berlin Heidelberg, 2008.
[6] Kausel, E., Lamb's problem at its simplest, *Proc. Royal Society A*, vol. 469 (2149), pp. 1-15, 2013.
[7] Rahman, M. and Michelitsch, T., A note on the formulae for the Rayleigh wave speed, *Wave motion*, vol. 43 (3), pp. 272-276, 2005.
[8] Ono, K., Calibration methods of acoustic emission sensors, *Materials*, vol. 9 (7), pp. 508, 2016.
[9] Regtien, P. P. L., Sensors of mechatronics, Elsevier Inc., Ed. 1, 2012.
[10] Johnson, L. R., Green's function for Lamb's problem, *Geophys. J. R. astr. Soc*., vol. 37, pp. 99-131, 1974.
[11] Lee, Y. H. and Oh, T., The measurement of P- S- And R wave velocities to evaluate the condition of reinforced and prestressed concrete slabs, *Advances in Materials Science and Engineering*, 14 pages, 2016.
[12] Rose, J. L., Waves in Plates, Ultrasonic guided waves in solid media, Cambridge University Press, New York, USA, 2014.